First-forbidden β decay: Meson-exchange enhancement of the axial charge at $A \sim 16$

E. K. Warburton
Brookhaven National Laboratory, Upton, New York 11973

I. S. Towner
AECL Research, Chalk River Laboratories, Chalk River, Ontario, Canada K0J 1J0

B. A. Brown
National Superconducting Cyclotron Laboratory and Department of Physics and Astronomy, Michigan State University, East Lansing, Michigan 48824

(Received 30 August 1993)

Calculations are presented for four relatively strong first-forbidden β decays in the region A = 11–16 in order to study the very large mesonic-exchange-current enhancement of the rank-zero components. The μ^- capture on ^{16}O is considered on the same footing. The wave functions utilized include up to $4\hbar\omega$ excitations. Two-body exchange-current matrix elements are calculated as well as one-body impulse-approximation matrix elements. The resultant enhancement factor that multiplies the impulse-approximation axial-charge matrix element is thereby determined by comparison to experiment to be $\epsilon_{\rm exp} = 1.61 \pm 0.03$ from three β^- decays and μ^- capture on ^{16}O, which is in excellent agreement with meson-exchange calculations in the soft-pion approximation.

PACS number(s): 21.60.Cs, 23.40.−s, 21.10.Dr, 27.20.+n

I. INTRODUCTION

This is one of several articles describing theoretical calculations of first-forbidden β decay observables and other related weak-interaction variables with as high accuracy as is currently possible. Recent results have been reported for A = 50 [1], and the A = 133–134 [2] and A = 205–212 [3] regions. Here we report on the four A = 11–16 decays of Fig. 1 and Table II. The main motive is to add understanding of the very large enhancement over the impulse approximation of the rank-zero (R0) axial-charge matrix element M_0^T observed especially in the lead region [10].

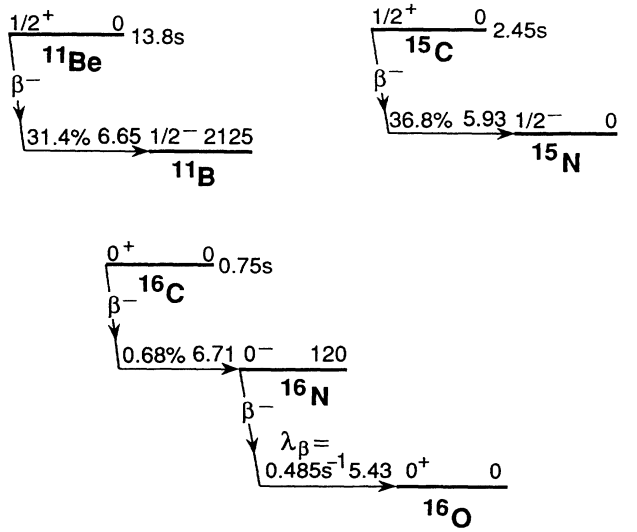

FIG. 1. The four $\Delta J = 0$ decays of interest to the present study. Each level is labeled by J^π and E_x (in keV). Each β^- branch is labeled by the percentage branching ratio (or decay rate) and $\log f_0 t$ value.

The four β decays of Fig. 1 are the known decays in light (A < 37) nuclei that are fast enough to provide potentially reliable information on the medium enhancement of M_0^T. In addition to these four decays, an important part of this study is a consideration of the inverse of ^{16}N(0$^-$) $\xrightarrow{\beta^-}$ ^{16}O(0$^+$), namely, μ^- capture on ^{16}O leading to the 0$^-$ first-excited state of ^{16}N with—for the first time—a calculational precision comparable to that routinely used in β-decay studies [11].

The light nuclei have always been and will continue to be the premier testing ground for our views on the structure of nuclei. Our main emphasis here will be on A = 16 nuclei. ^{16}O has a fascinating and complex structure since $0\hbar\omega$, $2\hbar\omega$, and $4\hbar\omega$ excitations are manifestly apparent among the low-lying levels. The $(0+2+4)\hbar\omega$ model of Brown and Green [12] was an early, successful, and important description of these states. Recently, we described a large-basis shell-model diagonalization of ^{16}O in a $(0+2+4)\hbar\omega$ basis and ^{16}N in a $(1+3)\hbar\omega$ basis [13]. Similar wave functions will be used in the ^{16}N(0$^-$) $\leftrightarrow$ ^{16}O(0$^+$) β^- and μ^- calculations. The β^- decays of ^{16}C, ^{15}C, and ^{11}Be will be treated in the more truncated $(1+3)\hbar\omega \rightarrow (0+2)\hbar\omega$ space (A = 11, 15) or the $(2+4)\hbar\omega \rightarrow (1+3)\hbar\omega$ space (^{16}C) with the effects of $4\hbar\omega$ or $5\hbar\omega$ added perturbatively.

In Sec. II we give a review of the shell-model interactions used in the present study. In Secs. III A and III B we describe the calculation of the one-body (impulse approximation) matrix elements, which enter in these rank-zero processes, and how they are combined to give theoretical rates. The two-body (meson exchange) matrix

elements are considered in Sec. III C. In Sec. IV we describe the $^{16}\mathrm{N}(0^-) \leftrightarrow {}^{16}\mathrm{O}(0^+)$ transitions and in Sec. V we take up the β^- decays of ^{15}C, ^{11}Be, and ^{16}C. Finally, in Sec. VI we discuss the conclusions concerning the enhancement factors for β^- and μ^- capture.

II. THE WAVE FUNCTIONS

Shell-model calculations were performed with the shell-model code OXBASH [14]. With OXBASH, spurious center-of-mass motion is removed by the usual method [15] of adding a center-of-mass Hamiltonian $H_{\mathrm{c.m.}}$ to the interaction. The shell-model studies start with the recently constructed interactions of Warburton and Brown [16], which are based on interactions for the $0p1s0d$ shells determined by a least-squares fit to 216 energy levels in the $A = 10$–22 region assuming no mixing of $n\hbar\omega$ and $(n+2)\hbar\omega$ configurations. The $0p1s0d$ part of the interaction cited in Ref. [16] as WBP results from a fit to two-body matrix elements (TBME) and single-particle energies (SPE) for the p shell and a potential representation of the $0p$-$(1s0d)$ cross-shell interaction. The WBP model space was expanded to include the $0s$ and $0f1p$ major shells by adding the appropriate $0f1p$ and cross-shell $1s0d$-$0f1p$ two-body matrix elements of the WBMB interaction [17] and all the other necessary matrix elements from the bare G-matrix potential of Hosaka, Kubo, and Toki [18]. The $0s$, $0f$, and $1p$ SPE were determined as described in Ref. [16]. Thus the WBP interaction is constructed in a similar manner to the Millener four-shell interaction described in Ref. [19], but reproduces the binding energies of low-lying $\geq 1\hbar\omega$ levels in the $A = 16$ region with 2–3 times greater accuracy.

Unless a complete model space is used for a given diagonalization, the wave functions can contain spurious components. For a $(0+2)\hbar\omega$ calculation in ^{16}O, the first four oscillator shells comprise a complete basis, while for a $(0+2+4)\hbar\omega$ calculation the first six shells must be included for completeness [13,20]. We began our shell-model studies by diagonalizing the $(0+2+4)\hbar\omega$ 0^+ $T = 0$ and $(1+3)\hbar\omega$ 0^--3^- $T = 1$ states of ^{16}O in model spaces comprising both the first six and first four oscillator shells. As discussed in Ref. [13], negligible difference was found in the wave functions and observables of interest between the calculations within these two model spaces. Thus the calculations reported here were performed in the four-shell model spaces — we emphasize that the results in six-shell model spaces would be essentially identical.

In Ref. [13] several methods for constructing the mixed $\hbar\omega$ spectra were explored, each of which gave a reasonable level scheme for $A = 16$. Since that work we have further explored the sensitivity of other observables such as the electron scattering form factors from the ground state of ^{16}O to 0^+, 2^+, and 4^+ excited states and the $M1$ decay of low-lying 1^+ $T = 1$ states [21]. We found that the method of lowering just the $4\hbar\omega$ configurations for the positive-parity states tends to produce too much mixing of the $4\hbar\omega$ components into those states around 12–18 MeV, which are known — from experimental observables — to be mostly $2\hbar\omega$. The gap method turns out to be better in this regard because it simultaneously lowers the $2\hbar\omega$ configurations with respect to the $4\hbar\omega$ configurations. The needed reduction of the $0p - 1s0d$ gap — initially $\Delta(0p$-$1s0d) = 11\,632$ keV — for the WBP interaction is 3.0 MeV, which means that the $2\hbar\omega$ states are shifted down by 6.0 MeV and the $4\hbar\omega$ states are shifted down by 12.0 MeV. It is worth noting, as discussed in Ref. [13], that the amount that the $4\hbar\omega$ configurations need to be lowered is essentially equal to the shift of the ground state in going from the $0\hbar\omega$ space to the $(0+2+4)\hbar\omega$ space. Thus the view can be taken that the shifts are not free parameters but with a given $\hbar\omega$ truncation can be determined self-consistently. When the negative-parity $T = 1$ states are treated in a $(1+3)\hbar\omega$ space it is perhaps reasonable to shift the $3\hbar\omega$ configurations down by 12.0 MeV and the $1\hbar\omega$ configurations down by 6.0 MeV, and doing so gives excellent agreement with experiment for the energies of these states relative to the positive-parity $T = 0$ states. Note that this is not the same as the pure gap method, which would involve shifts of 9.0 and 3.0 MeV for the $3\hbar\omega$ and $1\hbar\omega$ configurations, respectively. Nevertheless we will refer to this as the gap method since the structure of the negative-parity states are exactly the same in either case (since the structure only depends upon the 6.0-MeV shift difference between the $3\hbar\omega$ and $1\hbar\omega$ configurations). We refer to the results obtained with the fitted potential for all matrix elements and the gap method as WBP.

In addition, we have further explored the interaction $V^{2\hbar\omega}$ that mixes $n\hbar\omega$ and $(n+2)\hbar\omega$ configurations. In Ref. [13] this interaction (40 $0p$-$1s0d$ TBME) was generated from the potential obtained from the fit described above (WBP). However, since the core-polarization corrections may be different for $1\hbar\omega$ and $2\hbar\omega$ matrix elements, the use of a common potential may not be entirely correct. As an alternative we have explored [21] the use of the Bonn G matrix [22] for the mixing interaction $V^{2\hbar\omega}$. We find that the bare G matrix cannot reproduce the energy-level spectrum ^{16}O with any amount of $2\hbar\omega$ and/or $4\hbar\omega$ shift, but that the interaction was acceptable in this regard if it was renormalized by a factor of 0.8. Such a renormalization seems reasonable because the core-polarization corrections are found to reduce the average $V^{2\hbar\omega}$ matrix elements of the bare G matrix by about this amount [23]. We will refer to results obtained with $V^{2\hbar\omega}$ replaced by 0.8 times the Bonn G matrix as WBN. For this interaction the needed reduction in the $0p$-$1s0d$ gap was found to be 3.5 MeV so the $2\hbar\omega$ and $4\hbar\omega$ components are lowered by 7 and 14 MeV, respectively. As for the WBP interaction, the spirit of the gap method was retained for the odd-parity states in that the difference between the $3\hbar\omega$ and $1\hbar\omega$ shifts was set at 7 MeV. However the absolute shifts were arbitrarily set so as to minimize the difference in the experimental and theoretical excitation energies of the low-lying $T = 1$ quartet. This, of course, has no influence on the wave functions of the states.

The main reason for exploring the use of the Bonn $V^{2\hbar\omega}$ interaction was that the WBP interaction did not provide a satisfactory description of the electron scattering form

factors and of the $M1$ decay of the low-lying 1^+ $T = 1$ states. The WBN interaction does considerably better in this regard and, in fact, provides the most satisfactory description of these phenomena of any realistic interaction that we are aware of [21]. Thus the results given here for the WBN interaction are the preferred ones. The WBP results are given to provide a measure of the sensitivity to the interaction used.

III. THE WEAK INTERACTION PROCESSES

A. β^- and μ^- rates

Note that all the numerical results given in this subsection are relevant to $^{16}\mathrm{N} \leftrightarrow {}^{16}\mathrm{O}$. The relationship between experiment and theory is given here in a way that displays the similarity between $0^- \rightarrow 0^+$ β decay and $0^+ \rightarrow 0^-$ μ^- capture. It follows closely the treatments of Behrens and Bühring [11] for β decay and Nozawa, Kubodera, and Ohtsubo (NKO) [24] for both β^- decay and μ^- capture but especially the latter:

$$\Lambda_\beta = \frac{G^2}{2\pi^3}\frac{f_0}{\lambda_{Ce}{}^2}|M_0^\beta|^2, \tag{1a}$$

$$\Lambda_\mu = C_R\frac{G^2}{2\pi}\frac{\omega^2}{1+\omega/M_f}\frac{|\overline{\phi_{1s}(0)}|^2}{\lambda_{Ce}{}^2}\left[\frac{g_A(q^2)}{g_A(0)}\right]^2|M_0^\mu|^2. \tag{1b}$$

All quantities are in natural units $\hbar = \mathrm{c} = m_e = 1$. The unit of time is the second and of length λ_{Ce} — the electron Compton wavelength divided by 2π. The decay rate $\Lambda\ (= 1/\tau)$ has the units of sec^{-1}. G is the standard weak-interaction constant. The β-decay phase-space factor is

$$f = \int_1^{W_0} C(W)F(Z,W)(W^2-1)^{\frac{1}{2}}W(W_0-W)^2dW\ , \tag{2}$$

where $C(W)$ is the shape factor, $F(Z,W)$ is the Fermi function, W is the electron energy, and W_0 the total disintegration energy — both including the rest mass. The allowed phase-space factor, f_0 is given by the integral of Eq. (2) with the shape factor $C(W) = 1$. For a pure rank-zero (R0) decay as is involved here, $\overline{C(W)} = f/f_0 = |M_0^\beta|^2$ where the M_0^α ($\alpha \equiv \beta, \mu$) of Eq. (1) are combinations of matrix elements. We choose to give all matrix elements in fm; thus λ_{Ce} appears in Eq. (1). The axial-coupling constant $g_A(q^2)$ is a function of the four-momentum transfer q. For nuclear β decay $q = 0$ to a good approximation. We incorporate $g_A(0)$ ($\equiv g_A$) into the matrix elements. Hence it does not appear in Eq. (1a) and normalizes the q-dependent ratio $g_A(q^2)$ in Eq. (1b). In Eq. (1b), C_R is a second-order relativistic correction (see Appendix A), ω is the muon-neutrino energy, $(1+\omega/M_f)^{-1}$ is a recoil correction with M_f being the mass of the final nucleus, and $|\overline{\phi_{1s}(\mathbf{r})}|^2_{r=0}$ is the probability of finding the μ^- at the origin (see Appendix A):

$$|\overline{\phi_{1s}(0)}|^2 = \mathcal{R}_Z^2|\phi_{1s}(0)|^2_{\substack{\text{point}\\\text{nucleus}}} = \mathcal{R}_Z^2\frac{(Z\alpha m_\mu^r)^3}{\pi}. \tag{3}$$

TABLE I. Quantities needed in the evaluation of the $^{16}\mathrm{N}(0^-) \leftrightarrow {}^{16}\mathrm{O}(0^+)$ β^- and μ^- matrix elements and decay rates.

Quantity	Definition	Value	Ref.
α	Fine structure constant	1/137.036	[25]
λ_{Ce}	Electron Compton wavelength	386.159 fm	[25]
r_u	Uniform charge radius	3.537 fm	[26]
ξ	$\alpha Z/2r_u$	3.187	
γ	$[1-(\alpha Z)^2]^{1/2}$	0.99829	[11]
M_N	T_Z-averaged nucleon mass	1837.41	[25]
m_π	T_Z-averaged pion mass	270.128	[25]
m_μ	Muon mass	206.768	[25]
m_μ^r	Reduced muon mass	$0.99296m_\mu$	
$G^2/2\pi^3$	Weak-interaction factor (sec^{-1})	$[8851(20)]^{-1}$	[25]
ω	$m_\mu - \mathrm{Q}_\beta$	186.144	[27]
q^2	$-m_\mu^2 + 2m_\mu\omega$	$0.80051m_\mu^2$	[27]
q	Four-momentum transfer	184.998	[27]
g_A	$G_A/G\ [\equiv g_A(0)]$	1.261(4)	[25]
$g_A(q^2)/g_A(0)$	$[1+(q/M_N)^2]^{-1}$	0.9900	
Q_β	β-decay Q value	20.624(5)	[28]
$f_0/\lambda_{Ce}{}^2$	Phase-space factor	1.2574	[29]
$\frac{1}{\pi}(Z\alpha m_\mu^r)^3$	See Eq. (3)	548.10	
$\mathcal{R}_Z$	See Eq. (3)	0.91688	[24]
$g_P(q^2)/g_A(q^2)$	PCAC value	6.939	
E_μ(point nucleus)	γm_μ^r	204.961	[11]
E_K(point nucleus)	$(1-\gamma)m_\mu^r$	0.350	[11]
$(1+\omega/M_f)^{-1}$	Recoil correction	0.9937	
C_R	Relativistic correction	1.04	[24]

TABLE II. Experimental data for $\Delta J = 0$ first-forbidden decays in the $A \sim 16$ region. $t_{1/2}$ is the total half-life and b_r the branching ratio for the indicated final state. Q_β is defined in Eq. (14). $\overline{C(W)}$ is the average shape factor, $\equiv f/f_0$ [see Eq. (2)], and is given by $\overline{C(W)} = \sum_R B_1^{(R)}$ where $B_1^{(R)} \equiv |M_R^\beta|^2$ is the rank R β moment. For the $\frac{1}{2}^+ \to \frac{1}{2}^-$ transitions $R = 0,1$ and the measured $B_1^{(1)}/B_1^{(0)}$ listed in the sixth column is used to obtain M_0^β from $\overline{C(W)}$. For the $0^+ \leftrightarrow 0^-$ transitions this step is not necessary.

Transition	$t_{1/2}$ (s)	b_r (%)	Q_β (keV)	$\overline{C(W)}^{1/2}$ (fm)	$B_1^{(1)}/B_1^{(0)}$	M_0^β (fm)	Ref.
$^{11}\mathrm{Be}(\frac{1}{2}^+) \to {}^{11}\mathrm{B}(\frac{1}{2}^-)$	13.81(8)	31.4(18)	9381.3(60)	14.4(4)	<0.29	13.3(11)	[4,5]
$^{15}\mathrm{C}(\frac{1}{2}^+) \to {}^{15}\mathrm{N}(\frac{1}{2}^-)$	2.449(5)	36.8(8)	9771.68(80)	32.8(4)	0.185(13)	29.6(11)	[6]
$^{16}\mathrm{C}(0^+) \to {}^{16}\mathrm{N}(0^-)$	0.747(8)	0.68(10)	7891.7(43)	13.4(9)	0.00	13.4(9)	[7]
$^{16}\mathrm{N}(0^-) \to {}^{16}\mathrm{O}(0^+)$	1.429(56)	100.0(0)	10539.5(23)	58.4(11)	0.00	58.4(11)	[8,9]

In Eq. (3), m_μ^r is the reduced μ^- mass and $\mathcal{R}_Z$ is a correction factor obtained by solving the Dirac equation for the wave function of the muon in the field of a finite-charge distribution (see Appendix A). Parameter values (in natural units unless otherwise specified) relevant to $^{16}\mathrm{N}(0^-) \leftrightarrow {}^{16}\mathrm{O}(0^+)$ are given in Table I. Using these parameters we find

$$\Lambda_\beta = 1.4206 \times 10^{-4}|M_0^\beta|^2 = 0.485 \pm 0.019 \text{ sec}^{-1}, \quad (4a)$$

$$\Lambda_\mu = 0.1210|M_0^\mu|^2 = 1560 \pm 94 \text{ sec}^{-1}, \quad (4b)$$

where the experimental results on the right are taken from Refs. [9,30]. The experimental rates lead to the following experimental matrix elements:

$$M_0^\beta = 83.90[\Lambda_\beta(s^{-1})]^{\frac{1}{2}} = 58.4 \pm 1.1 \text{ fm}, \quad (5a)$$

$$M_0^\mu = 2.874[\Lambda_\mu(s^{-1})]^{\frac{1}{2}} = 113.5 \pm 3.4 \text{ fm}. \quad (5b)$$

Results for the β-decay matrix elements for the other three cases of interest are given in Table II. It is these experimental matrix elements that we will compare to theory. We write M_0^β and M_0^μ in the form

$$M_0^\beta = [M_0^T + M_\pi^\beta + a_S^\beta M_0^S] = [M_0^T \epsilon^\beta + a_S^\beta M_0^S], \quad (6)$$

$$M_0^\mu = [a_T^\mu M_0^T + M_\pi^\mu - a_S^\mu M_0^S] = [a_T^\mu M_0^T \epsilon^\mu - a_S^\mu M_0^S],$$

where the M_π^α are the two-body meson-exchange current (mec) matrix elements defined in Sec. III C below. When Eqs. (5) and (6) are used to compare experiment and theory, it is conventional to extract values of ϵ^α that are required to reproduce experiment, and these will be referred to as $\epsilon_{\mathrm{exp}}^\alpha$. The calculated values for ϵ^α based upon these equations together with the calculated two-body M_π^α discussed in Sec III C will be referred to as $\epsilon_{\mathrm{mec}}^\alpha$.

Our evaluation of the β-decay rate follows the rigorous and accurate treatment of Behrens and Bühring [11]. In writing the expression for M_0^β in Eq. (6) small terms included in the first-order treatment have been neglected. However, for the decays in question these terms contribute less than 0.2% to M_0^β. In the Behrens-Bühring treatment the a_S^β of Eq. (6) is given by [11,32,27,31]

$$a_S^\beta = \tfrac{1}{3}(Q_\beta + 1) + \xi r_S^\beta = 7.208 + 3.187 r_S^\beta, \quad (7)$$

where Q_β is dimensionless (in units of the electron mass) and the numerical results apply to the $^{16}\mathrm{N} \to {}^{16}\mathrm{O}$ decay. Note the r_S^β and the a_S^α and a_T^α of Eqs. (6) and (7) are positive-definite quantities so that the contributions of M_0^T and M_0^S add destructively in forming M_0^β and constructively in forming M_0^μ.

The a_S^μ and a_T^μ of Eq. (6) and r_S^β of Eq. (7) are defined as ratios of matrix elements evaluated with extra radial factors to the normal matrix elements. The radial dependencies for μ^- capture are given explicitly in Appendix A. In Eq. (7) the ratio r_S^β is insensitive to the wave functions used. Approximate values of a_S^β are $\approx$ 7.80, 8.52, 7.45, and 9.40 for the decays of $^{11}\mathrm{Be}$, $^{15}\mathrm{C}$, $^{16}\mathrm{C}$, and $^{16}\mathrm{N}$, respectively. Note however that all a_T^α and a_S^α are calculated explicitly for the wave functions at hand.

B. The one-body contribution

Our concern here is with the one-body (impulse approximation) matrix elements of the rank-zero (R0) axial current. These are the matrix elements of the R0 member of the spin-dipole operator and of the helicity operator γ_5, which is commonly called the timelike component of the axial current, or the axial charge. With γ_5 replaced by its nonrelativistic limit (good to order $1/M_N$) the single-particle matrix elements (with the relative phase appropriate to β decay) are [32–35]

$$M_0^S(j_i j_f) = g_A\sqrt{3}\langle j_f|||ir[C_1, \boldsymbol{\sigma}]^0\boldsymbol{\tau}|||j_i\rangle C_{TJ}, \quad (8a)$$

$$M_0^T(j_i j_f) = -g_A\sqrt{3}\langle j_f|||\tfrac{i}{M_N}[\boldsymbol{\sigma}, \boldsymbol{\nabla}]^0\boldsymbol{\tau}|||j_i\rangle C_{TJ}\lambda_{Ce}{}^2, \quad (8b)$$

where

$$C_{TJ} = \frac{(-1)^{T_f - T_{zf}}}{[2(2J_i+1)]^{1/2}} \begin{pmatrix} T_f & 1 & T_i \\ -T_{zf} & \Delta T_z & T_{zi} \end{pmatrix}, \quad (9)$$

and

$$C_1 = \sqrt{\frac{4\pi}{3}} Y_1, \tag{10}$$

and where $\lambda\!\!\!^{-}_{Ce}$ — the electron Compton wavelength divided by 2π — is incorporated into Eq. (8b) so that both matrix elements have the dimensions of fm. The j_i and j_f are a short-hand notation for all quantum numbers needed to label the single-particle states. In Eq. (9), the J_i and T dependencies result from the reduced matrix elements in a spin and isospin space and $\sqrt{2}$ is from the definition of the isospin operator. The radial integrals contained in the matrix elements of Eq. (8) were evaluated by numerical integration; however it is useful to keep in mind that the two operators are Hermitian conjugates, which for harmonic-oscillator radial wave functions results in the identity

$$M_0^T(j_i j_f) = -\left[\frac{E_{\rm osc}}{m_e c^2}\right] M_0^S(j_i j_f), \qquad \text{for HO.} \tag{11}$$

Equation (11) is approximately true for the more realistic radial wave functions (see below) used in the present study. The usual shell-model procedure is followed of combining the single-particle matrix elements $M_R^\alpha(j_i j_f)$ with one-body transition densities $D_R^{(1)}(j_i j_f)$ via

$$M_R^\alpha = \sum_{j_i j_f} \mathcal{M}_R^\alpha(j_i j_f) = \sum_{j_i j_f} D_R^{(1)}(j_i j_f) M_R^\alpha(j_i j_f), \tag{12}$$

where the subscript R denotes the rank of the operator ($R = 0$ in this study). The one-body transition densities given by

$$D_R^{(1)}(j_i j_f) = \frac{\langle J_f T_f || [a_{j_i}^\dagger \otimes \tilde{a}_{j_f}]^{\Delta T \Delta J} || J_i T_i \rangle}{[(2\Delta J + 1)(2\Delta T + 1)]^{\frac{1}{2}}} \tag{13}$$

contain all the information on the initial and final many-body wave functions. The $J_i T_i$ and $J_f T_f$ are short-hand notations for all quantum numbers needed to describe the many-body wave functions and ΔT,ΔJ are multipolarities of the one-body operator, which in our case has $\Delta T = 1$ and $\Delta J = R = 0$.

In the previous calculations for heavier nuclei [1–3], the single-particle matrix elements were augmented by multiplicative renormalization factors $q_\alpha(j_i j_f)$ that represented first-order core-polarization effects. In the present calculation the model space is large enough to include all possible first-order core-polarizations, and so the one-body operators appropriate to bare nucleons are used.

The $M_R^\alpha(j_i j_f)$ and also the two-body matrix elements described in Sec. III C are calculated with a combination of harmonic-oscillator (HO) and Woods-Saxon (WS) wave functions. The WS parameters were determined by extrapolation of results obtained by least-squares fits to nuclear charge distributions for ^{12}C and ^{16}O [36]. In this procedure the separation energies were fixed as described below and the orbit occupancies were taken from $(0+2+4)\hbar\omega$ wave functions for ^{16}O [13] and ^{12}C [21]. For HO wave functions, we first found values of $\hbar\omega$ for ^{12}C and ^{16}O that reproduced the root-mean-square charge radii, $\langle r^2 \rangle^{\frac{1}{2}}$, with these orbit occupancies. For ^{16}O, with $\langle r^2 \rangle^{\frac{1}{2}} = 2.730$ fm [36], the result is $\hbar\omega = 13.60$ MeV as opposed to 13.16 MeV, which is obtained assuming an ^{16}O closed shell. Values of $\hbar\omega$ for $A = 11$ and 15 were obtained from the $A = 12$ and 16 values assuming a linear dependence on A.

The WS results depend on the separation energies $S(n)$ for the β^- parent state and $S(p)$ for the daughter. These are related by

$$S(p) - S(n) = Q_\beta - 0.782 \text{ MeV}, \tag{14}$$

where $Q_\beta - 0.782$ MeV is the difference in binding energies of the initial and final states. The separation energies for a particular common parent state with excitation energy E_x in the $(A-1,Z-1)$ core are then

$$S(n) = \Delta E_b(n) + E_x - E_i, \tag{15a}$$

$$S(p) = \Delta E_b(p) + E_x - E_f, \tag{15b}$$

where E_i and E_f are the excitation energies of the initial and final states in the $(A, Z-1)$ and (A, Z) nuclei, respectively, and $\Delta E_b(n)$ is the difference in binding energies of the ground state of the initial nucleus and the $(A-1, Z-1)$ core nucleus, i.e., the neutron separation energy for the ground states, and similarly for $\Delta E_b(p)$.

The main effect of small separation energies is to increase the relative magnitude of the "tail" of the radial wave function. As the separation energies increase, the difference between WS and HO wave functions lessens, and becomes insignificant compared to our knowledge of the wave functions. Thus we use HO wave functions for all single-particle transitions except those allowed for $\nu(1s0d) \rightarrow \pi(0p)$; i.e., all others have large effective values of E_x and thus of $S(n)$ and $S(p)$.

The method developed by Millener [38] and adopted to a similar calculation [10] for ^{206}Tl $\rightarrow$ ^{206}Pb was used to estimate the effective value of E_x, $\langle E_x(j) \rangle$, to use in Eq. (15). This method involves an inclusive calculation of the spectroscopic amplitudes for neutron pickup from the initial state and proton pickup from the final state to all possible core states and an evaluation of the effective excitation energy of the core states from a consideration of these amplitudes and the resulting dependence of the matrix elements on E_x. In this determination all core-state excitation energies greater than 10 MeV were fixed at 10 MeV. The results for the rank-zero $\nu 1s_{1/2} \rightarrow \pi 0p_{1/2}$ and $\nu 0d_{3/2} \rightarrow \pi 0p_{3/2}$ transitions — the two allowed $\nu(1s0d) \rightarrow \pi(0p)$ transitions — are given in Table III. The $\langle E_x(j) \rangle$ of Table III are calculated with the WBP interaction with the lowest allowed $n\hbar\omega$ wave functions for each of the three nuclei involved in each of the four cases. In contrast to these simple wave functions, we present results in this study calculated for model spaces as complex as $(1+3)\hbar\omega \rightarrow (0+2+4)\hbar\omega$. The question might well be asked as to the relevance of Table III to these more complex — and hopefully more realistic — calculations. To address this question the procedure was applied to the $\nu 1s_{1/2} \rightarrow \pi 0p_{1/2}$ single-particle component

TABLE III. Summary of results for the neutron and proton separation energies $S(n)$ and $S(p)$ for use with Woods-Saxon wave functions. All energies in the last seven columns are in keV.

Transition	j	$\Delta E_b(n)$	$\Delta E_b(p)$	E_i	E_f	$\langle E_x \rangle$	$S(n)$	$S(p)$
$^{16}\mathrm{N}(0^-) \rightarrow {}^{16}\mathrm{O}(0^+)$	$\frac{1}{2}$	2491	12128	120	0	0	2371	12128
	$\frac{3}{2}$					6324	8695	18452
$^{16}\mathrm{C}(0^+) \rightarrow {}^{16}\mathrm{N}(0^-)$	$\frac{1}{2}$	4251	11480	0	120	25	4276	11385
	$\frac{3}{2}$					4267	8518	15627
$^{15}\mathrm{C}(\frac{1}{2}^+) \rightarrow {}^{15}\mathrm{N}(\frac{1}{2}^-)$	$\frac{1}{2}$	1218	10208	0	0	0	1218	10208
	$\frac{3}{2}$					8746	9964	18954
$^{11}\mathrm{Be}(\frac{1}{2}^+) \rightarrow {}^{11}\mathrm{B}(\frac{1}{2}^-)$	$\frac{1}{2}$	504	11228	0	2125	70	574	9173
	$\frac{3}{2}$					7013	7517	16116

in the $^{16}\mathrm{N} \rightarrow {}^{16}\mathrm{O}$ rank-zero decay with typical $(1+3)\hbar\omega$ and $(0+2+4)\hbar\omega$ wave functions for $^{16}\mathrm{N}(0^-)$ and $^{16}\mathrm{O}(0^+)$, respectively, and with typical $(0+2)\hbar\omega$ wave function for the $^{15}\mathrm{N}$ $\frac{1}{2}^-$ states. In a $(0+2)\hbar\omega$ space, there are 265 $^{15}\mathrm{N}$ $\frac{1}{2}^-$ states, 41 of which are spurious. The value of $\langle E_x(j) \rangle$ found for the 224 nonspurious states is 32 keV, in close agreement with the value of zero keV associated with the simple calculation of Table III.

For the $\nu 0d_{3/2} \rightarrow \pi 0p_{3/2}$ transitions the large values of $\langle E_x(j) \rangle$ mean that the matrix elements are not sensitive to its value, in fact, one might just as well (in ignorance) use HO wave functions for the $j = \frac{3}{2}$ transitions and we do so for the calculation of the one-body matrix elements M_0^S and M_0^T and the two-body matrix element M_β^π and M_μ^π.

C. The two-body soft-pion contribution

Towner [39] has recently made an investigation of the one-pion exchange contribution to single-particle matrix elements of the axial charge in (closed shell $\pm$ 1) nuclei from $A \sim 16$–208. Towner's results indicate that for $A \sim 16$ the soft-pion diagram [40,41] alone gives an adequate representation of the meson exchange and so we only consider this term. The soft-pion contribution was incorporated into the shell-model calculations in the manner described for the similar parity-nonconserving (PNC) matrix element [42]. The general expression for the soft-pion contribution is a sum of the product of a two-body transition density $D_0^{(2)}(j_1 j_2 J T j_3 j_4 J T')$ and a two-body meson-exchange matrix element:

$$M_\pi^\beta = -G_{\mathrm{soft}\pi} C_{TJ} \sum_{\substack{j_1 \le j_2 \\ j_3 \le j_4 \\ JTT'}} D_0^{(2)}(j_1 j_2 J T j_3 j_4 J T') \langle j_1 j_2 J T ||| \hat{g}(r_r) i(\boldsymbol{\sigma_1} + \boldsymbol{\sigma_2}) \cdot \hat{\boldsymbol{r}}_r (\boldsymbol{\tau_1} \times \boldsymbol{\tau_2}) Y_\pi(x_\pi) ||| j_3 j_4 J T' \rangle, \quad (16)$$

where $x_\pi = m_\pi r_r$ with $\boldsymbol{r}_r = \boldsymbol{r_1} - \boldsymbol{r_2}$, $Y_\pi(x_\pi) = (1 + 1/x_\pi) e^{-x_\pi}/x_\pi$ and $\hat{g}(r_r)$ is a short-range correlation (SRC) function. The SRC used in this work was $\hat{g}(r_r) = 1 - j_0(q_c r_r)$ with $q_c = 3.93\ \mathrm{fm}^{-1}$ [39]. We will also compare results obtained with this SRC and with the simple cut-off factor $\theta(r_r - d)$ for which $\hat{g}(r_r) = 1$ for $r_r > d$ and 0 for $r_r \le d$. The soft-pion coupling constant is defined as

$$G_{\mathrm{soft}\pi} = \frac{\sqrt{2}}{8\pi} \frac{g_{\pi NN}^2}{g_A} \frac{m_\pi^2}{M_N^2} \lambda_{Ce} = 69.74\ \mathrm{fm}, \quad (17)$$

where we have used $g_{\pi NN} = 13.684$ [22]. The two-body transition density of Eq. (16) is given by

$$D_0^{(2)}(j_1 j_2 J T j_3 j_4 J T') = \frac{\langle J_f T_f ||| \{ [a_{j_1}^\dagger \otimes a_{j_2}^\dagger]^{JT} \otimes [\bar{a}_{j_3} \otimes \bar{a}_{j_4}]^{JT'} \}^{\Delta J = 0, \Delta T = 1} ||| J_i T_i \rangle}{[(2\Delta J + 1)(2\Delta T + 1)(1 + \delta_{j_1 j_2})(1 + \delta_{j_3 j_4})]^{1/2}}. \quad (18)$$

As for the other shell-model calculations, the evaluation of M_π^β involved four oscillator shells and the use of mixed HO and WS radial wave functions. Our results for single-particle transitions are identical to the soft-pion results of Towner [39]. Here we consider more complicated transitions. The computer program used is formulated in terms of harmonic-oscillator wave functions. Our method of allowing Woods-Saxon radial wave functions is to expand

TABLE IV. Soft-pion enhancement factors for simple transitions encountered in $^{16}\mathrm{N}(0^-) \rightarrow {}^{16}\mathrm{O}(0^+)$ calculated with HO wave functions ($\hbar\omega = 13.60$ MeV) for two different short-range correlation functions. WS results are also given for the $\nu 1s_{1/2} \rightarrow \pi 0p_{1/2}$ and $\nu 0d_{3/2} \rightarrow \pi 0p_{3/2}$ transitions. Note that the last three transitions have an ^{16}O $0\hbar\omega$ core.

Initial state	Final state	$\epsilon^{\beta}_{\mathrm{mec}}$		$\epsilon^{\mu}_{\mathrm{mec}}$	
		$1 - j_0(3.93r_r)$	$\theta(r_r - 0.71)$	$1 - j_0(3.93r_r)$	$\theta(r_r - 0.71)$
		$1\hbar\omega \rightarrow 0\hbar\omega$			
$\nu 1s_{1/2}\pi(0p_{1/2})^{-1}$	$(0s)^4(0p)^{12}$	1.549[a]	1.488[a]	1.510[a]	1.425[a]
		1.523[b]	1.467[b]	1.509[b]	1.427[b]
$\nu 0d_{3/2}\pi(0p_{3/2})^{-1}$	$(0s)^4(0p)^{12}$	1.418[a]	1.383[a]	1.449[a]	1.387[a]
		1.428[b]	1.379[b]	1.457[b]	1.393[b]
		$1\hbar\omega \rightarrow 2\hbar\omega$			
$\nu 1s_{1/2}\pi(0p_{1/2})^{-1}$	$\nu(1s_{1/2})\nu(0s_{1/2})^{-1}$	1.405	1.367	1.417	1.361
$\nu 1s_{1/2}\pi(0p_{1/2})^{-1}$	$\nu(1s_{1/2})^2\pi(0p_{1/2})^{-2}$	1.525	1.458	1.488	1.406
$\nu 0d_{3/2}\pi(0p_{3/2})^{-1}$	$\nu(0d_{3/2})^2\pi(0p_{3/2})^{-2}$	1.331	1.293	1.356	1.306
		$1s0d \rightarrow 0f1p$			
$0d_{5/2}$	$0f_{5/2}$	1.226	1.201	1.253	1.212
$0d_{3/2}$	$1p_{3/2}$	1.488	1.430	1.436	1.360
$1s_{1/2}$	$1p_{1/2}$	1.305	1.264	1.310	1.248

[a]HO results.
[b]WS results.

the appropriate WS radial wave function in terms of HO wave functions (up to 10 terms). As explained in Sec. III B, we use WS wave functions for the $\nu 1s_{1/2} \rightarrow \pi 0p_{1/2}$ transition but use HO wave functions to evaluate the rest. As for the one-body matrix element, μ^- capture differs from β decay in that the analogous M^{μ}_{π} to the M^{β}_{π} of Eq. (16) should be evaluated with the factor a^{μ}_T [$\approx j_0(\omega r)$] of Eq. (A17) of the Appendix inserted. Thus a dependence on $\boldsymbol{r}$ [$\equiv \frac{1}{2}(\boldsymbol{r_1} + \boldsymbol{r_2})$] as well as on $\boldsymbol{r_r}$ is introduced. This dependence is approximated by retaining terms up to order ω^2 with the result that the replacement

$$(\boldsymbol{\sigma_1} + \boldsymbol{\sigma_2}) \cdot \hat{\boldsymbol{r}}_r \rightarrow (\boldsymbol{\sigma_1} + \boldsymbol{\sigma_2}) \cdot \hat{\boldsymbol{r}}_r - \tfrac{1}{6}\omega^2(r^2 + \tfrac{1}{4}r_r^2)(\boldsymbol{\sigma_1} + \boldsymbol{\sigma_2}) \cdot \hat{\boldsymbol{r}}_r + \tfrac{1}{6}\omega^2(\boldsymbol{r} \cdot \boldsymbol{r}_r)(\boldsymbol{\sigma_1} - \boldsymbol{\sigma_2}) \cdot \hat{\boldsymbol{r}}_r \qquad (19)$$

was made in Eq. (16) to obtain M^{μ}_{π} [43].

The relative contributions of M^{β}_{π} to M^T_0 is formulated in terms of the ϵ^{β} parameter defined in Eq. (6). It is informative to consider the values of $\epsilon^{\beta}_{\mathrm{mec}}$ obtained for simple configurations. Evaluations with HO and WS wave functions are collected in Table IV for two different SRC factors. It is seen that $\epsilon^{\beta}_{\mathrm{mec}}$ has a fairly strong state dependence. Because of this state dependence and because the two-body and one-body matrix elements have different dependencies on the nuclear wave functions, Eq. (16) or an equivalent expression must be used for a rigorous evaluation of $\epsilon^{\beta}_{\mathrm{mec}}$. However, a useful approximation is

$$\epsilon^{\beta}_{\mathrm{mec}} \approx \frac{\sum_{j_i j_f} D^{(1)}_R(j_i j_f)\epsilon^{\beta}_{\mathrm{mec}}(j_i j_f)M^T_0(j_i j_f)}{\sum_{j_i j_f} D_R(j_i j_f)M^T_0(j_i j_f)}, \qquad (20)$$

with a similar expression for $\epsilon^{\mu}_{\mathrm{mec}}$. Comparison shows that this approximation — used with the results listed in Table IV to represent the $\epsilon^{\beta}_{\mathrm{mec}}(j_i j_f)$ — underestimates $\epsilon^{\beta}_{\mathrm{mec}}$ by ~5%. Nevertheless, this approximation is useful because the evaluation of Eq. (16) takes an unusually large amount of computer time. In comparisons of different diagonalizations and tests of different radial forms or SRC factors we make use of Eq. (20).

IV. RESULTS FOR $^{16}\mathrm{N}(0^-) \leftrightarrow {}^{16}\mathrm{O}(0^+)$

As a first orientation, consider the four decays of Table II in successive degrees of model-space complexity. The simplest of these is the "single-particle" approximation in which only the $0p_{1/2}$ and $1s_{1/2}$ degrees of freedom are allowed. Next allow for mixing within a single major-oscillator shell but keep only the lowest possible $\hbar\omega$ configurations, e.g., $1\hbar\omega \leftrightarrow 0\hbar\omega$ for the $^{16}\mathrm{N} \leftrightarrow {}^{16}\mathrm{O}$ transitions. In this approximation the WBP and WBN interactions are equivalent. The results for the two calculations are compared in Table V. First we observe that in all cases there is a significant reduction in going from the simple configuration to the major-oscillator configuration. This is primarily due to a destructive interference between the $\nu 1s_{1/2} \leftrightarrow \pi 0p_{1/2}$ and $\nu 0d_{3/2} \leftrightarrow \pi 0p_{3/2}$ terms in Eq. (12).

The next level of approximation allows for those terms which enter in the next order in a perturbation expansion. For $1\hbar\omega \rightarrow 0\hbar\omega$ transitions, this means including $2\hbar\omega$ admixtures in the final state since these connect directly to the $1\hbar\omega$ initial state; $3\hbar\omega$ admixtures in the initial state are not included in this order because they

TABLE V. Results obtained for restricted model spaces. All were obtained with the Woods-Saxon potential.

Transition	Model space	M_0^T	M_0^S
$^{11}\mathrm{Be}(\frac{1}{2}^+) \rightarrow {}^{11}\mathrm{B}(\frac{1}{2}^-)$	Single particle	34.3	−1.59
	$1\hbar\omega \rightarrow 0\hbar\omega$	18.0	−0.97
$^{15}\mathrm{C}(\frac{1}{2}^+) \rightarrow {}^{15}\mathrm{N}(\frac{1}{2}^-)$	Single particle	47.3	−2.20
	$1\hbar\omega \rightarrow 0\hbar\omega$	35.9	−1.76
$^{16}\mathrm{C}(0^+) \rightarrow {}^{16}\mathrm{N}(0^-)$	Single particle	81.1	−3.12
	$2\hbar\omega \rightarrow 1\hbar\omega$	26.8	−1.22
$^{16}\mathrm{N}(0^-) \rightarrow {}^{16}\mathrm{O}(0^+)$	Single particle	81.1	−3.12
	$1\hbar\omega \rightarrow 0\hbar\omega$	62.1	−2.70

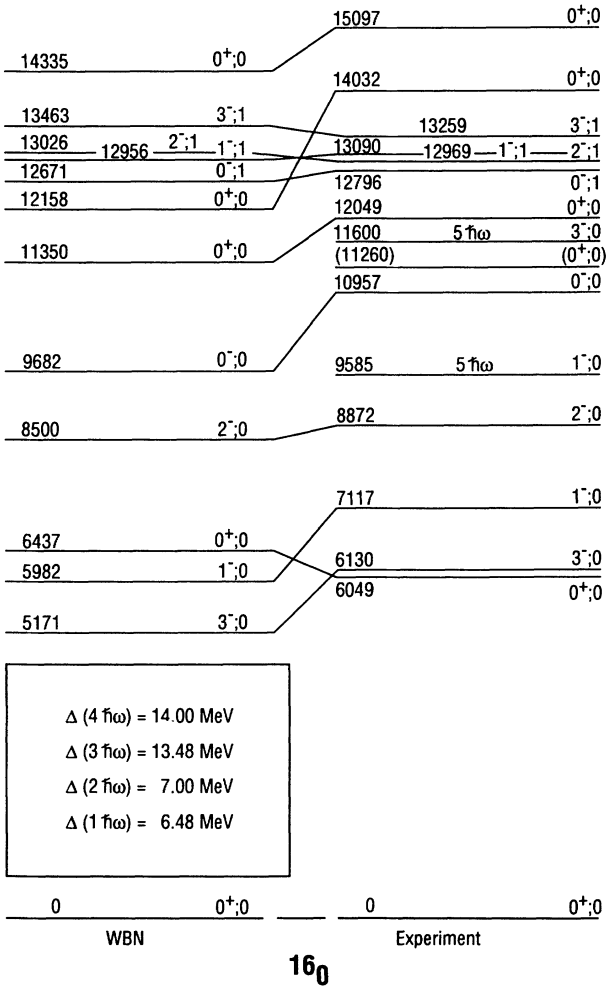

FIG. 2. Comparison of partial WBN and experimental level schemes of ^{16}O. The experimental energies and spin-parity assignments are from Ref. [53]. The theoretical levels were calculated with the indicated downward shifts to the different $n\hbar\omega$ components relative to the unshifted $0\hbar\omega$ components. The centroid of the $1\hbar\omega + 3\hbar\omega$ shifts was set so as to minimize the difference in excitation energies for the yrast $T = 1$ odd-parity quartet. The other shifts were set as discribed in the text. The levels included in the figure are the lowest five 0^+ $T = 0$ level, the odd-parity $T = 1$ quartet, and all $T = 0$ odd-parity levels below 12-MeV excitation. There is no WBN counterpart for the known predominantly $5\hbar\omega$ experimental 1^- and 3^- states at 9585 and 11 600 keV, respectively. The experimental 0^+ level at 11 260 keV is tentative [53]. We assume it does not exist.

do not directly connect to the $0\hbar\omega$ final state and it is inconsistent to include them without also including $4\hbar\omega$ terms in the final state. A consistent higher-order calculations involves $(1+3)\hbar\omega \rightarrow (0+2+4)\hbar\omega$ transitions and is only possible at present for ^{16}N decay, which we now consider.

The model-space dimensions for ^{16}N 0^- in a $(1+3)\hbar\omega$ model space and ^{16}O 0^+ in a $(0+2+4)\hbar\omega$ model space are 713 and 4255, respectively. The gap reduction for the WBP interaction is 3.0 MeV. The lowest five ^{16}O 0^+ $T = 0$ states are calculated to lie at 0.00, 6.59, 10.77, 11.69, and 14.25 MeV with the 6.59-MeV state predominately (88%) $4\hbar\omega$. The structure of the ground state is 43.2% $0\hbar\omega$, 43.2% $2\hbar\omega$, and 13.6% $4\hbar\omega$. The lowest two 0^- $T = 1$ states occur at 12.38 and 17.37 MeV and the structure of the lowest 0^- and 2^- $T = 1$ states are both (coincidentally) 71.1% $1\hbar\omega$ and 28.9% $3\hbar\omega$.

A partial WBN level scheme is compared to experiment in Fig. 2. The gap reduction for the WBN interaction is 3.5 MeV. The structure of the ground state is 34.9% $0\hbar\omega$, 46.7% $2\hbar\omega$, and 18.4% $4\hbar\omega$. The 6.44-MeV 0_2^+ state is predominantly (87%) $4\hbar\omega$. The structure of the lowest 0^- $T = 1$ state is 64.5% $1\hbar\omega$ and 35.5% $3\hbar\omega$.

The β^- R0 and R2 decays of the 0^- and 2^- states of ^{16}N are illustrated in Fig. 3. Results for the $^{16}\mathrm{N}(0^-) \rightarrow$

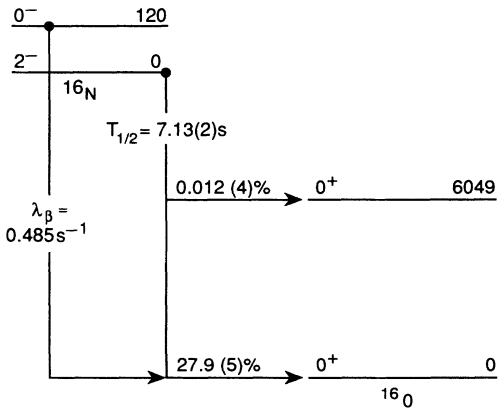

FIG. 3. Experimental data for R0 and R2 β^- decays of the 0^- and 2^- states of ^{16}N. Each level is labeled by J^π and E_x (in keV). The R0 decay is labeled by the decay rate and the R2 decays is labeled by the total half-life and the individual branching ratios.

TABLE VI. Results obtained from the $(1+3)\hbar\omega \rightarrow (0+2+4)\hbar\omega$ calculations for ^{16}N(0^-) $\rightarrow$ ^{16}O(0^+) R0 β decay. The $\epsilon^{\beta}_{\rm exp}$ were obtained from Eq. (6) using the experimental value of $M^{\beta}_0 = 58.4 \pm 1.1$. The $\epsilon^{\beta}_{\rm mec}$ were obtained using the calculated matrix element M^{β}_{π} as discussed in Sec. III C with the $[1-j_0(3.93r_r)]$ short-range correlation.

Interaction	WS/HO	M^T_0	a^{β}_S	M^S_0	$\epsilon^{\beta}_{\rm exp}$	$\epsilon^{\beta}_{\rm mec}$
WBP	HO	49.9	10.01	−2.59	1.69(2)	1.63
WBN	HO	56.6	9.49	−2.26	1.41(2)	1.60
WBP	WS	41.7	9.37	−2.58	1.98(3)	1.61
WBN	WS	48.8	9.36	−2.26	1.63(2)	1.62

TABLE VII. Results obtained from the $(1+3)\hbar\omega \rightarrow (0+2+4)\hbar\omega$ calculations for ^{16}O(0^+) $\rightarrow$ ^{16}N(0^-) μ^- capture. The $\epsilon^{\mu}_{\rm exp}$ were obtained from Eq. (6) using the experimental value of $M^{\mu}_0 = 113.5 \pm 3.4$. The $\epsilon^{\mu}_{\rm mec}$ was obtained using the calculated matrix element M^{μ}_{π} as discussed in Sec. III C with the $[1-j_0(3.93r_r)]$ short-range correlation and the PCAC value of g_p of Table III.

Interaction	WS/HO	$a^{\mu}_T\ M^T_0$	$a^{\mu}_S\ M^S_0$	$\epsilon^{\mu}_{\rm exp}$	$\epsilon^{\mu}_{\rm mec}$
WBP	HO	46.5	65.9	1.02(7)	1.60
WBN	HO	51.5	57.2	1.09(7)	1.59
WBP	WS	36.8	56.9	1.54(9)	1.61
WBN	WS	41.8	48.8	1.55(8)	1.59

TABLE VIII. Results obtained from the $(1+3)\hbar\omega \rightarrow (0+2+4)\hbar\omega$ calculations for ^{16}N(2^-) $\rightarrow$ ^{16}O(0^+_n) R2 β decay.

n	Expt	Interaction	WS/HO	$M^z_2(0^+_n)$
1	3.04(2)	WBP	HO	2.91
		WBN	HO	2.61
		WBP	WS	2.93
		WBN	WS	2.63
2	1.09(18)	WBP	HO	0.96
		WBN	HO	1.03
		WBP	WS	0.96
		WBN	WS	1.03

TABLE IX. WBN ^{16}N(0^-) $\rightarrow$ ^{16}O(0^+) results for the $D^{(1)}_0(j_i j_f)$ and matrix elements of Eq. (12) calculated with WS wave functions for the dominant line five and HO wave functions for the other entries as discussed in the text.

νj_i	πj_f	$D^{(1)}_0(j_i j_f)$	$M^{\beta}_S(j_i j_f)$	$\mathcal{M}^{\beta}_S(j_i j_f)$	$M^{\beta}_T(j_i j_f)$	$\mathcal{M}^{\beta}_T(j_i j_f)$
$0p\ 1/2$	$0s\ 1/2$	0.0019	3.6473	0.0069	−105.7247	−0.1988
$1p\ 1/2$	$0s\ 1/2$	−0.0016	0.0000	0.0000	−0.0187	−0.0000
$0d\ 3/2$	$0p\ 3/2$	0.0504	6.9739	0.3515	−184.9045	−9.3192
$0s\ 1/2$	$0p\ 1/2$	0.0211	3.6139	0.0762	105.8366	2.2310
$1s\ 1/2$	$0p\ 1/2$	0.7857	−3.1164	−2.4486	73.0472	57.3932
$0f\ 5/2$	$0d\ 5/2$	−0.0062	10.1179	−0.0627	−269.3061	1.6697
$0p\ 3/2$	$0d\ 3/2$	−0.0424	6.9820	−0.2963	185.8391	−7.8870
$1p\ 3/2$	$0d\ 3/2$	0.0037	−4.4158	−0.0162	117.5352	0.4302
$0p\ 1/2$	$1s\ 1/2$	−0.0243	−3.1224	0.0759	−83.1269	2.0216
$1p\ 1/2$	$1s\ 1/2$	−0.0036	4.9370	−0.0178	−131.4311	0.4732
$0d\ 5/2$	$0f\ 5/2$	−0.0003	10.1179	−0.0030	269.3061	−0.0808
$0d\ 3/2$	$1p\ 3/2$	0.0013	−4.4158	−0.0057	−117.5352	−0.1516
$0s\ 1/2$	$1p\ 1/2$	0.0000	0.0000	0.0000	0.0187	−0.0000
$1s\ 1/2$	$1p\ 1/2$	0.0169	4.9370	0.0834	131.4311	2.2199
		Total		−2.2564		48.8014

$^{16}O(0^+)$ R0 β decay are given in Table VI and those for the $^{16}O(0^+) \rightarrow {}^{16}N(0^-)$ R0 μ^- capture are given in Table VII. As a further test of the wave functions, we compare with experiment [6,44] in Table VIII R2 results for the $^{16}N(2^-) \rightarrow {}^{16}O(0^+)$ unique first-forbidden β decays, which are simpler and better understood [13,32] than the R0 decays. For example, no appreciable mesonic contribution to R2 transitions is expected. As in Ref. [13] the good agreement between theory and experiment for these R2 transitions provides some evidence for the correctness of our wave functions.

The decompositions of M_0^T and M_2^z obtained with the WBP interaction for the R0 and R2 β decays to the ^{16}O ground state into the four possible $n\hbar\omega \rightarrow (n\pm1)\hbar\omega$ components are shown in Fig. 4. The various $n\hbar\omega$ contributions follow the classic pattern found for deexcitation of $E1$-like particle-hole configurations in a previous study of

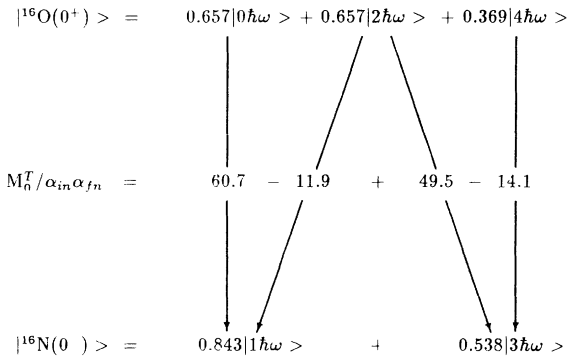

FIG. 4. Schematic showing the contributions of $n\hbar\omega \rightarrow (n\pm1)\hbar\omega$ transitions to the $^{16}N \leftrightarrow {}^{16}O$ R0 M_0^T matrix element in the $0^- \leftrightarrow 0_1^+$ transition (a) and the R2 M_2^z matrix element in the $2^- \leftrightarrow 0_1^+$ transition (b). Both are calculated with WS wave functions and the WBP interaction. $\alpha_{\rm in}$ and $\alpha_{\rm fn}$ are the amplitudes of the various $\hbar\omega$ components in the initial and final states, respectively.

first-forbidden decays in the $A = 40$ region [32]. In particular, the $1\hbar\omega \rightarrow 0\hbar\omega$ and $3\hbar\omega \rightarrow 2\hbar\omega$ matrix elements and the $1\hbar\omega \rightarrow 2\hbar\omega$ and $3\hbar\omega \rightarrow 4\hbar\omega$ matrix elements are closely equal and the latter two are out of phase with the former. The detailed composition of the $\mathcal{M}_0^\alpha$ of Eq. (12) for the $^{16}N(0^-) \rightarrow {}^{16}(0^+)$ β^- decay is given in Table IX.

V. RESULTS FOR ^{15}C, ^{11}Be, AND ^{16}C β^- DECAY

In this section we will only consider results obtained with the WBN interaction using the gap method and mixed WS and HO single-particle radial wave functions. We will confine our comparison of experiment and theory to a quotation of the M_0^α and the value of $\epsilon_{\rm exp}^\beta$, which when combined with the calculated M_0^α reproduces experiment. In all three cases, the calculated $\epsilon_{\rm mec}^\beta$ differ negligibly from that calculated for ^{16}N decay.

A. $^{15}C(\frac{1}{2}^+) \rightarrow {}^{15}N(\frac{1}{2}^-)$

The dimension $D(J = \frac{1}{2})$ of the J-matrix for the $T = \frac{3}{2}$, $J^\pi = \frac{1}{2}^+$ states of ^{15}C is 2369 in the four-shell $(1+3)\hbar\omega$ model space. For the $T = \frac{1}{2}$, $J^\pi = \frac{1}{2}^-$ states of ^{15}N $D(\frac{1}{2})$ is 23 762 for a $(0+2+4)\hbar\omega$ calculation and 265 for a $(0+2)\hbar\omega$ calculation. We can easily manage the ^{15}C $(1+3)\hbar\omega$ and ^{15}N $(0+2)\hbar\omega$ calculations but the $(0+2+4)\hbar\omega$ calculation is beyond our present resources. An attempt to truncate the ^{15}N $(0+2+4)\hbar\omega$ calculation by restricting the $4\hbar\omega$ part to 4p-4h (4 particle–4 hole) excitations between the $0p$ and $1s0d$ shells failed because the low-lying states in this truncation were highly spurious. This is in contrast to similar calculations performed for the 0^+ states of ^{16}O [13] and ^{12}C [21]. (The low-lying 0^+ states in the latter calculations were nearly spurious free.) However, the importance of the $4\hbar\omega$ component in the ^{16}O ground state suggests a similar importance in ^{15}N and we would like to include an estimation of its effect. Thus a $(1+3)\hbar\omega \rightarrow (0+2)\hbar\omega$ calculation was made with the effects of adding a $4\hbar\omega$ term to ^{15}N estimated by assuming the same amplitude of $4\hbar\omega$ in the ^{15}N ground state as in ^{16}O (see Fig. 4) and assuming

$$M(3\hbar\omega \rightarrow 4\hbar\omega) \approx \frac{M(1\hbar\omega \rightarrow 2\hbar\omega)}{M(1\hbar\omega \rightarrow 0\hbar\omega)} M(3\hbar\omega \rightarrow 2\hbar\omega), \tag{21}$$

where $M[(n \pm 1)\hbar\omega \rightarrow n\hbar\omega]$ is the specific component, such as in Fig. 4, of either M_0^T or M_0^S. Thus Eq. (21) quantifies our observations on the systematics of Fig. 4.

A value of $\Delta_{3\hbar\omega} = -8.50$ MeV was determined for the ^{15}C $(1+3)\hbar\omega$ calculation by a least-squares matching to the eleven experimental even-parity $A = 15$ $T = \frac{1}{2}$ energy levels for $J \leq \frac{5}{2}$ states below 11 MeV, the yrast $T = \frac{3}{2}$ $\frac{1}{2}^+$, and $\frac{5}{2}^+$ states, and the yrast $T = \frac{1}{2}$ $\frac{13}{2}^+$ state. The value of $\Delta_{2\hbar\omega}$ used in the ^{15}N calculation was determined as -8.30 MeV from a similar consideration of the $A = 15$

odd-parity spectrum.

The results are $M_0^T = 27.66$ fm, $M_0^S = 1.53$ fm, $\epsilon^\beta_{\rm exp} = 1.54 \pm 0.04$ (uncertainty from experiment only).

B. ^{11}Be($\frac{1}{2}^+$) $\rightarrow$ ^{11}B($\frac{1}{2}^-$)

The calculation for ^{11}Be($\frac{1}{2}^+$) $\rightarrow$ ^{11}B($\frac{1}{2}^-$) follows the procedure just described for ^{15}C($\frac{1}{2}^+$) $\rightarrow$ ^{15}N($\frac{1}{2}^-$) with the reliance on the $(0+2+4)\hbar\omega$ ^{16}O 0_1^+ wave function in the latter case changed to a similar reliance on the $(0+2+4)\hbar\omega$ ^{12}C 0_1^+ wave function. The $D(\frac{1}{2})$ for the $(1+3)\hbar\omega \rightarrow (0+2)\hbar\omega$ calculation are 5674 and 1063, respectively. Little of a definite nature is known about the $2\hbar\omega$ and $3\hbar\omega$ states of ^{11}B and ^{11}Be. Thus the values of $\Delta_{2\hbar\omega}$ and $\Delta_{3\hbar\omega}$ used in the calculations were assumed to be equal and were obtained by linear interpolation between values found for ^{10}B, ^{12}C, and ^{15}N. The resulting value is -4.00 MeV.

The effect of the $4\hbar\omega$ component in ^{11}B was considerably less than the similar effect in ^{15}N simply because the ^{12}C ground-state wave function has only 1.86% $4\hbar\omega$ as opposed to 13.6% in ^{16}O.

The results are $M_0^T = 14.05$ fm, $M_0^S = 1.10$ fm, $\epsilon^\beta_{\rm exp} = 1.56 \pm 0.08$ (uncertainty from experiment only).

C. ^{16}C(0^+) $\rightarrow$ ^{16}N(0^-)

After considering ^{16}C(0^+) $\rightarrow$ ^{16}N(0^-) in detail we conclude that the calculated matrix elements are unusually sensitive to the details of the calculation and thus not suitable for a determination of $\epsilon^\beta_{\rm exp}$. To understand this, first consider the simple $2\hbar\omega \rightarrow 1\hbar\omega$ calculation of Table V. In the case of ^{16}C the reduction of the M_0^α in going from the simple single-particle configuration to the major-oscillator configuration is unusually large and interaction dependent, because of the competition between the $0d_{5/2}^2$ and $1s_{1/2}^2$ configurations in the ^{16}C ground state. As a consequence of this, the configuration in ^{16}C, which is responsible for the destructive $\nu 0d_{3/2} \rightarrow \pi 0p_{3/2}$ term (but which accounts for only about 0.3% of the ^{16}C wave function), results in a $\sim$50% reduction of the matrix elements.

Now consider the mixing of $2\hbar\omega$ and $4\hbar\omega$ components. A $(2+4)\hbar\omega$ calculation — which has $D(0^+) = 4055$ — was performed. The same decrease of the $0p$-$1s0d$ energy gap, 3.5 MeV, for the $T = 2$ 0^+ states was used as was applied for the $T = 0$ 0^+ states. We find the first 10 states (i.e., all that were examined) to be >44% $4\hbar\omega$ with, e.g., the ground state being 55% $2\hbar\omega$ and 45% $4\hbar\omega$. The $(0_1^+, 2)$ excitation energy in ^{16}O was 22.2 MeV as compared to the experimental value of 24.52 MeV. The prominance of the $4\hbar\omega$ component may seem surprising at first sight; however, if a weak-coupling approximation such as that of Bansal and French [37] is used to estimate the binding energies of ^{14}C$\otimes^{18}$O, and ^{12}C$\otimes^{20}$O, one finds that these energies are nearly degenerate so that which lies lowest and the energy gap between them depends on the details of the interaction. Thus it is not surprising that the $(2+4)\hbar\omega$ mixing is large and unusually sensitive to the details of the calculation.

Because of these sensitivities we believe that the ^{16}C decay is primarily a test of the wave functions and does not provide a good measure of the mesonic-exchange-current enhancement. This extreme wave function sensitivity for ^{16}C also applies to similar R0 decays of ^{17}N and ^{18}Ne [38]. We do not consider this decay any further in this study.

VI. DISCUSSION AND SUMMARY

We comment first on the value of the enhancement factor for timelike axial-charge matrix elements deduced from a comparison of the impulse approximation with experiment, $\epsilon^\alpha_{\rm exp}$. It is evident from Tables VI and VII that the value of $\epsilon^\alpha_{\rm exp}$ is strongly dependent on the single-particle radial wave function used to describe the $\nu 0s_{1/2} \rightarrow \pi 0p_{1/2}$ transition. The WS result is strongly preferred since it provides the most realistic estimate of these radial wave functions. The HO results are included to give some indication of the sensitivity of the results to the radial form. We will not consider the HO results further. Likewise, the results of the WBN interaction are strongly preferred over those of the WBP interaction for the reasons stated in Sec. II. Again, the WBP results are listed to give an indication of the sensitivity to the shell-model interaction and will not be considered further.

In addition to the dependence on single-particle wave functions and shell-model interactions, there is a further dependence we have not yet considered; namely, the dependence of the μ^- capture rate on the pseudoscalar coupling constant g_p (see Appendixes A and B). For the WBN interaction with WS wave functions the dependence on g_p can be expressed as

$$\epsilon^\mu_{\rm exp} = 1.55 + 0.085(g_p - 6.939). \qquad (22)$$

In the evaluation of the β^- R0 matrix element M_0^β the contributions of M_0^T and M_0^S add destructively while they add constructively in M_0^μ [see Eq. (6)]. This relative phasing results in less model dependence for the determination of $\epsilon^\mu_{\rm exp}$ than for that of $\epsilon^\beta_{\rm exp}$ and it has often been asserted that, for this reason, μ^- capture provides a considerably more reliable determination of $\epsilon_{\rm exp}$ than β decay. However, the uncertainty in g_p (see Appendix B) completely negates this conclusion; from Eq. (22) we see that the range of g_p of $\sim$7–12 allowed by analysis of radiative μ^- capture (see Appendix B) corresponds to a range in $\epsilon_{\rm exp}$ values of 1.55–2.00 — a range large enough to offset the aforementioned advantage.

Our adopted value for $\epsilon_{\rm exp}$ follows from a consideration of the results for the three β^- decays that were analyzed. The average of the three results (1.54 ± 0.04, 1.56 ± 0.08, 1.63 ± 0.02) quoted for $\epsilon_{\rm exp}$ is 1.61 ± 0.03 and this is the result we shall adopt. We note that the μ^- capture result of 1.55 ± 0.08 (for the PCAC value of g_p) is in good accord with this value especially if the small difference between $\epsilon^\beta_{\rm mec}$ and $\epsilon^\mu_{\rm mec}$ of $\sim$0.02 is added to the $\epsilon^\mu_{\rm exp}$ value.

The previous most ambitious calculation of the pro-

cesses in question were the $(1+3)\hbar\omega \rightarrow (0+2)\hbar\omega$ calculation of Warburton [45] for the four β^- decays of Table II and the $(1+3)\hbar\omega \leftrightarrow (0+2+4)\hbar\omega$ results of Haxton and Johnson [20] for the $^{16}\mathrm{N}(0^-) \leftrightarrow {}^{16}\mathrm{O}(0^+)$ β^- and μ^- processes. The calculations of Warburton [45], using the MK interaction, result in an average $\epsilon^{\beta}_{\mathrm{exp}}$ of 1.64 for the decays of Table II, in good agreement with the present result of 1.61. Haxton and Johnson obtained results very close to the present results given for the WBP interaction with WS wave functions [46]. This is not surprising to us since we had found that the $V^{2\hbar\omega}$ derived from the Kuo bare G matrix [23] — the $V^{2\hbar\omega}$ of the MK interaction used by Haxton and Johnson — has quite similar properties to the $V^{2\hbar\omega}$ of the WBP potential. It is the change to the Bonn potential for $V^{2\hbar\omega}$ that gives us a substantial improvement in the agreement of experiment and theory.

The theoretical values for the enhancement factors, $\epsilon^{\beta}_{\mathrm{mec}}$ and $\epsilon^{\mu}_{\mathrm{mec}}$, calculated from a meson-exchange model in the soft-pion approximation are very close to our adopted experimental value and show very little model dependence varying from 1.60 to 1.63 and 1.59 to 1.61, respectively, depending on the choice of interaction and single-particle wave functions. This insensitivity has been noted previously in work on parity nonconserving interactions [47] and follows because the two-body matrix element can be represented quite well by an effective one-body matrix element proportional to $\boldsymbol{\sigma}\cdot\boldsymbol{p}$ — and thus to M_0^T — consequently the ratio of the two-body to one-body matrix elements is not sensitive to nuclear structure. However, as discussed by Towner [39], the results from meson-exchange models are dependent on the choice of a short-range correlation function. This is particularly true for the short-range operators discussed in [39] originating in heavy-meson exchange. In this paper, we have only considered the long-range pion-exchange operators evaluated in the soft-pion approximation for which the sensitivity to SRC is somewhat less. Some sample calculations are given in Table IV. For the all-important $\nu 1s_{1/2} \rightarrow \pi 0p_{1/2}$ transition the use of the $\theta(r_r - 0.71)$ form reduces $\epsilon^{\alpha}_{\mathrm{mec}}$ by a factor 0.96 compared to the $1-j_0(3.93r_r)$ form and the other transitions in this table have similar ratios. In the full calculation for both β decay and μ^- capture ($\alpha \equiv \beta, \mu$), the reduction factor is 0.95–0.96. In what follows we will only discuss calculations using the SRC function $\hat{g}(r_r) = 1 - j_0(q_c r_r)$ with $q_c = 3.93$ fm^{-1} [39].

As discussed above and in Appendix B, the μ^- capture results depend on the pseudoscalar coupling constant, g_p. This dependence offers the opportunity to extract a value for g_p from a comparison of the β^- and μ^- results. For the WBN interaction and WS wave functions with the $1-j_0(q_c r_r)$ SRC — our preferred selection — the adopted value $\epsilon^{\beta}_{\mathrm{exp}} = 1.61 \pm 0.03$ (which we assume to yield $\epsilon^{\mu}_{\mathrm{exp}} = 1.59 \pm 0.04$) and use of Eq. (22) leads to $g_p = 7.4 \pm 0.5$ consistent with the PCAC value. Note that the uncertainties assigned to ϵ_{exp} and g_p reflect experiment only and do not include any estimate of the uncertainty associated with the theoretical analysis.

Finally we compare these results for the $A = 16$ mass region with our recent results for the $A = 132$ [2] and $A = 208$ [3] regions. As noted in Sec. III B the calculations in the heavier mass regions are further complicated by the need to introduce core-polarization corrections. These corrections depend sensitively on the strength of the residual interaction used in their evaluation and in particular on the strength of the tensor force which, according to Brown and Rho [48], is liable to medium modifications similar to those proposed for the pion-decay constant [49,50]. With a weak tensor force, the enhancement factors deduced are $\epsilon^{\beta}_{\mathrm{exp}}(A = 132) = 1.82 \pm 0.07$ and $\epsilon^{\beta}_{\mathrm{exp}}(A = 208) = 1.79 \pm 0.04$. With strong tensor forces, values of $\epsilon^{\beta}_{\mathrm{exp}}$ some 10% larger are obtained. Thus there is clearly more enhancement in heavy nuclei than in light nuclei, which are characterized by our current value $\epsilon_{\mathrm{exp}}(A = 16) = 1.61 \pm 0.03$. To quantify the mass dependence we define a ratio

$$r = \frac{\epsilon_{\mathrm{exp}}(A = 208) - 1}{\epsilon_{\mathrm{exp}}(A = 16) - 1}, \tag{23}$$

which for weak tensor forces has a value 1.30 ± 0.10 and for strong tensor forces a value 1.49 ± 0.11. The calculated value of this ratio from meson-exchange models obtained by Towner [39] is 1.38, which is approximately midway between the experimental results obtained assuming weak and strong tensor forces. There is still some room for further sources of enhancement in the heavier nuclei such as medium modification of the nucleon mass and of the pion-decay constant used in the soft-pion approximation as proposed by Kubodera and Rho [50] on the basis of a scaling in the effective chiral Lagrangian discussed by Brown and Rho [49]. But the compelling need for such an alternative explanation that was thought present a few years ago now appears to be absent.

ACKNOWLEDGMENTS

We thank S. Nozawa, K. Kubodera, and H. Ohtsubo for their generous and expert help in understanding the details of their study of $^{16}\mathrm{N} \leftrightarrow {}^{16}\mathrm{O}$, Ref. [24]. We especially thank H. Ohtsubo for providing us with his computer program for solving the Dirac equation for the wave function of a K-shell muon and for instructions in its use. Research was supported in part by the U.S. Department of Energy under Contract No. DE-AC02-76CH00016 with Brookhaven National Laboratory and in part by the National Science Foundation under Grant No. PHY-90-17077 with Michigan State University. B.A.B. would also like to acknowledge support from the Humboldt Foundation.

APPENDIX A: μ^- CAPTURE

Nozawa, Kubodera, and Ohtsubo [24] — referred to as NKO — developed an approach to μ^- capture on $^{16}\mathrm{O}$, which can be used with numerical solutions of the Dirac equation. In this appendix we wish to make the bridge between the μ^- capture formalism developed by NKO and numerical results found by combining their solution of the Dirac equation with our shell-model wave func-

tions. In essence this means we will give explicit expressions for the radial dependence of the matrix elements, which will then be evaluated by numerical integration.

Our expression for the μ^- capture rate [Eq. (1b)] is

$$\Lambda_\mu = C_R \frac{G^2}{2\pi} \frac{\omega^2}{1+\omega/M_f} \frac{|\overline{\phi_{1s}(0)}|^2}{\lambda_{Ce}{}^2} \left[\frac{g_A(q^2)}{g_A(0)}\right]^2 |M_0^\mu|^2. \quad \text{(A1)}$$

In order to evaluate relativistic effects, NKO applied a Foldy-Wouthuysen transformation first to order $1/M_N$ and then to order $1/M_N^2$. They showed that the terms of order $1/M_N^2$ contribute $\sim 2\%$ (constructively) to the μ^- capture matrix element M_0^μ. We will calculate Λ_μ to first order in $1/M_N$ but include a multiplicative factor of C_R (=1.04) in Eq. (A1) to compensate for the $1/M_N^2$ term in our evaluation of M_0^μ.

In Eq. (A1) $|\overline{\phi_{1s}(0)}|^2$ is the probability of finding a K-shell muon at the origin and is just $1/4\pi$ times the square of the large component of the muon wave function $G_{-1}(r)$ evaluated at $r=0$. For a point nucleus [11]

$$G_{-1}^{(p)}(r) = \left[\frac{(1+\gamma)\lambda}{\Gamma(1+2\gamma)}\right]^{1/2} r^{-1}(2\lambda r)^\gamma e^{-\lambda r}, \quad \text{(A2a)}$$

$$F_{-1}^{(p)}(r) = -\frac{\alpha Z}{1+\gamma} G_{-1}^{(p)}(r), \quad \text{(A2b)}$$

where $F_{-1}(r)$ is the smaller component of the muon wave function and $\gamma = [1-(\alpha Z)^2]^{1/2}$. When appropriate, we use the superscripts (p) and (g) on G_{-1} and F_{-1} to denote a point nucleus and a nucleus with a Gaussian charge distribution, respectively. In Eq. (A2)

$$\lambda = \left[(m_\mu^r + E_\mu)(m_\mu^r - E_\mu)\right]^{1/2}, \qquad E_\mu = m_\mu^r \gamma, \quad \text{(A3)}$$

where E_μ is the energy eigenvalue for the K shell for a point nucleus. The approximation often used for $G_{-1}^{(p)}(r)$ is

$$G_{-1}^{(p)}(r) \overset{Z\to 0}{\longrightarrow} 2(\alpha Z m_\mu^r)^{3/2}. \quad \text{(A4)}$$

Thus we take the probability of finding the muon at the origin (in the unit volume $\lambda\!\!\!^{-3}_{Ce}$) to be

$$|\overline{\phi_{1s}(r)}|^2_{r=0} = \frac{1}{4\pi}[G_{-1}(0)]^2 = \frac{1}{\pi}(\alpha Z m_\mu^r)^3 R_Z^2, \quad \text{(A5)}$$

where R_Z is a correction evaluated by solving the Dirac equation for a realistic extended nuclear-charge distribution.

We use NKO's solution of the Dirac equation. These authors used a Gaussian charge distribution $\rho(r)$ given by

$$\rho(r) = \rho_0\left[1 + a(r/r_0)^2\right] e^{-(r/r_0)^2}, \quad \text{(A6)}$$

with $r_0 = 1.83$ fm and $a = 1.45$. This charge distribution gives $G_{-1}^{(g)}(0) = 0.91688$ and large and small components of the muon wave function, which are well reproduced by the phenomenological power expansion

$$G_{-1}^{(g)}(r) = \sum_{n=0}^{10} a_n r^n, \qquad F_{-1}^{(g)}(r) = \sum_{n=0}^{10} b_n r^n, \quad \text{(A7)}$$

with the coefficients given in Table X.

The Foldy-Wouthuysen transformation to first order in $1/M_N$ leads to a one-body operator for μ^- capture given by [24]

$$J_\mu^{1-\text{body}} = [i\mathbf{A}\cdot\hat{\mathbf{r}}L^+(r) + A_0\mathcal{L}^-(r) + i\tilde{A}\mathcal{L}^+(r)]\boldsymbol{\tau} \quad \text{(A8)}$$

with radial functions

$$L^\pm(r) = \frac{1}{\sqrt{2}}[G_{-1}(r)j_1(\omega r) \pm F_{-1}(r)j_0(\omega r)], \quad \text{(A9)}$$

$$\mathcal{L}^\pm(r) = \frac{1}{\sqrt{2}}[G_{-1}(r)j_0(\omega r) \pm F_{-1}(r)j_1(\omega r)], \quad \text{(A10)}$$

and operators

$$i\mathbf{A}\cdot\hat{\mathbf{r}} = -g_A\boldsymbol{\sigma}\cdot\hat{\mathbf{r}}, \quad \text{(A11)}$$

$$A_0 = ig_A\boldsymbol{\sigma}\cdot\mathbf{P}/2M_N, \quad \text{(A12)}$$

$$\tilde{A} = m_\mu G_p \boldsymbol{\sigma}\cdot\mathbf{k}/2M_N. \quad \text{(A13)}$$

Here $j_0(\omega r)$ and $j_1(\omega r)$ are spherical Bessel functions representing the neutrino wave functions. Note that $\mathbf{P}$ and $\mathbf{k}$ depend on the momenta of the initial and final nucleons, $\mathbf{P} = \mathbf{p}_i + \mathbf{p}_f$ and $\mathbf{k} = \mathbf{p}_i - \mathbf{p}_f$, which occur in combination with radial functions $\mathcal{L}(r)$. In the Fourier transform to coordinate space these momenta transform into derivative operators according to the replacement rules

$$\mathbf{P}\mathcal{L}(r) \to -i\hat{\mathbf{r}}\frac{\partial}{\partial r}\mathcal{L}(r) - 2i\mathcal{L}(r)\boldsymbol{\nabla}, \quad \text{(A14)}$$

$$\mathbf{k}\mathcal{L}(r) \to i\hat{\mathbf{r}}\frac{\partial}{\partial r}\mathcal{L}(r). \quad \text{(A15)}$$

Then, upon evaluating the partial derivatives, we find

TABLE X. The power-series coefficients of Eq. (A7) that reproduce the Dirac wave function for the charge distribution of Eq. (A6) with an absolute error $< 5\times10^{-6}$ for $r < 10$ fm. The numbers in square brackets are powers of 10.

n	a_n	b_n
0	+ 9.16882[−01]	+ 0.00000[−00]
1	+ 3.56365[−06]	− 8.29499[−03]
2	− 4.51773[−03]	+ 3.49933[−04]
3	+ 1.06662[−04]	− 3.02963[−04]
4	− 5.80056[−05]	+ 3.88561[−04]
5	+ 7.30971[−05]	− 1.40780[−04]
6	− 2.20053[−05]	+ 2.59785[−05]
7	+ 3.29970[−06]	− 2.77866[−06]
8	− 2.76786[−07]	+ 1.73880[−07]
9	+ 1.24699[−08]	− 5.87474[−09]

expressions for the full matrix element evaluated to order $1/M_N$. In terms of the operators defined in Eq. (1) and the normalization imposed by the expression for the μ^- capture rate in Eq. (A1), the one-body operator becomes

$$J_\mu^{1-\text{body}} = a_T^\mu M_0^T - a_S^\mu M_0^S \tag{A16}$$

with

$$a_T^\mu = \frac{1}{G_{-1}(0)}[G_{-1}(r)j_0(\omega r) - F_{-1}(r)j_1(\omega r)], \tag{A17}$$

$$a_S^\mu = \frac{1}{rG_{-1}(0)}[[g_{\text{large}} + \delta_{\text{large}}(r)]G_{-1}(r)j_1(\omega r) \tag{A18}$$

$$+ [g_{\text{small}} + \delta_{\text{small}}(r)]F_{-1}(r)j_0(\omega r)],$$

where in our notation M_0^T and M_0^S are equivalent to NKO's notation $-\frac{1}{M_N}\boldsymbol{\sigma}\cdot\boldsymbol{\nabla}\boldsymbol{\tau}_-$ and $\boldsymbol{\sigma}\cdot\mathbf{r}\,\boldsymbol{\tau}_-$. In Eq. (A18)

$$g_{\text{large}} = \frac{3}{\omega}g_\mu = 1 - \frac{\omega}{2M_N}(g_p - 1) = 0.6969,$$

$$g_{\text{small}} = 1 + \frac{1}{2M_N}[2m_\mu(g_p - 1) + \omega(g_p + 1)] = 2.0753,$$

$$\delta_{\text{large}}(r) = \frac{1}{2M_N}[V(r) + E_K](g_p + 1),$$

$$\delta_{\text{small}}(r) = \frac{-1}{2M_N}\left[[V(r) + E_K](g_p - 1) + \frac{4}{r}(g_p + 1)\right],$$

and $g_p = m_\mu G_p(q^2)/g_A(q^2)$ is the pseudoscalar coupling constant. In these expressions, E_K is the K-shell μ^- binding energy [$\equiv (1-\gamma)m_\mu$ for a point nucleus], and $V(r)$ is a potential evaluated from the charge distribution used to calculate $G_{-1}(r)$ and $F_{-1}(r)$. The potential is

$$V(r) = \frac{1}{r}\int_0^r \rho(x)x^2dx + \int_r^\infty \rho(x)x\,dx \tag{A19}$$

with

$$\int_0^\infty \rho(r)dr = \alpha Z. \tag{A20}$$

The approximate solution designated "simple" by NKO corresponds to the limits

$$\begin{aligned} &G_{-1}(r) \to G_{-1}(0), \\ &F_{-1}(r) \to 0, \qquad \text{"simple" solution} \\ &V(r) + E_K \to 0. \end{aligned} \tag{A21}$$

We have arranged the terms in Eqs. (A17) and (A18) so that it is easily apparent that in this limit Eq. (A16) reduces to

$$J_\mu^{1-\text{body}}(\text{simple}) = j_0(\omega r)M_0^T + g_\mu\frac{3}{\omega r}j_1(\omega r)M_0^S. \tag{A22}$$

The terms in $\delta_{\text{small}}(r)$ and $\delta_{\text{large}}(r)$ give small contributions ($\leq 2\%$). As pointed out by NKO, the g_{small} term gives a contribution of order 10%.

APPENDIX B: PSEUDOSCALAR COUPLING CONSTANT

For semileptonic weak processes, the $V-A$ structure of the weak interaction is modified by the induced weak currents that arise from the presence of the strong interaction. For the axial current one common parametrization is

$$A_\mu = i\overline{u}(p_f)\left(g_A(q^2)\gamma_\mu\gamma_5 - \frac{G_p(q^2)}{2M}\,q_\mu \not{q}\gamma_5\right)u(p_i)\frac{\tau^a}{2}, \tag{B1}$$

where the strong interactions have renormalized the axial-vector coupling constant $g_A(q^2)$ from a bare value of unity and introduced a pseudoscalar term with coupling constant $G_p(q^2)$. Here $\overline{u}(p_f)$ and $u(p_i)$ are spinors representing the final and initial state nucleons, q is the momentum transfer, and τ^a is the Pauli isospin matrix with the superscript a representing the Cartesian index $x \pm iy$. If, additionally, a constraint is imposed on Eq. (B1), namely, that the axial current shall be partially conserved, the PCAC condition, then a relation between $G_p(q^2)$ and $g_A(q^2)$ can be established.

One model for the weak axial current of a nucleon, that satisfies by construction the PCAC condition, is one of meson dominance discussed by Towner [39]. In this model, the g_A term in Eq. (B1) originates in the axial current being mediated by the A_1 meson in its interaction with a nucleon, while the G_p term is mediated by the π meson. The chiral Lagrangian that is used to describe the meson-nucleon interaction preferentially chooses pseudovector coupling for πNN vertices. Hence there is a pseudovector form, $q_\mu \not{q}\gamma_5$, to the G_p term in Eq. (B1). However for on-mass-shell nucleons, the use of the Dirac equation can transform this equation into one with pseudoscalar coupling, $q_\mu\gamma_5$. Using this meson dominance model, Towner [39] obtains

$$G_p(q^2) = \frac{2Mg_A(q^2)}{q^2 + m_\pi^2}\left(1 - \frac{m_\pi^2}{m_A^2}\right). \tag{B2}$$

The last factor, which tends to unity in the limit $m_\pi/m_A \to 0$, is not usually present in the literature. To get this result from the chiral Lagrangian the Weinberg relation is used relating the A_1-meson mass to the ρ-meson mass: $m_A^2 = 2m_\rho^2$. With an experimental ρ-meson mass of 768.1 MeV, this leads to an A_1-meson mass of $m_A = 1086.3$ MeV. On the other hand, neutrino-nucleon scattering analyzed using $g_A(q^2) = g_A(0)m_A^2/(m_A^2 + q^2)$ deduce that $m_A \simeq 950$ MeV. Thus there is some small uncertainty on the precise value of m_A to use in Eq. (B2). We will take $m_A = 950$ MeV and use for the nucleon and

pion masses their isospin averages to obtain for the dimensionless quantity

$$g_p \equiv \frac{m_\mu G_p(q^2)}{g_A(q^2)} = \frac{2Mm_\mu}{q^2+m_\pi^2}\left(1-\frac{m_\pi^2}{m_A^2}\right) = 6.939 \quad \text{(B3)}$$

for $q^2 = 0.8m_\mu^2$. This is the value recorded in Table I.

The pseudoscalar coupling constant, g_p, is the least well measured of all the nucleon weak-interaction coupling constants. Its value in Eq. (B3) typically represents a free-nucleon value and could be modified when that nucleon is embedded in a nuclear medium. The most promising way to determine g_p experimentally is in radiative μ^- capture [51]. The branching ratio for radiative μ^- capture relative to ordinary (nonradiative) μ^- capture is particularly sensitive to g_p. However the extraction of g_p from nuclear radiative μ^- capture measurements requires a model calculation of the inclusive nuclear response function and this piece of the determination is not yet under good control. For example, the most precise measurement for the ^{16}O branching ratio [51] yields values of $g_p = 7.3 \pm 0.9$, 9.1 ± 0.9, and 13.6 ± 1.9 when compared with three different recent calculations of the nuclear response. Nevertheless there is a hint here that the value of g_p in ^{16}O is larger than the PCAC value, Eq. (B3). A similar statement can be made for ^{12}C. For heavier nuclei, analyzed using a Fermi-gas model calculation of the nuclear response, the indication [51,52] is that g_p falls below the PCAC value and even quenches to zero for nuclei as heavy as Pb.

For ^{16}O, there is an alternative way to obtain g_p; namely, from the first-forbidden 0^- to 0^+ β transition from ^{16}N and the inverse μ^- capture on ^{16}O, the reactions under study in this paper. Gagliardi *et al.* [8] using the model calculations of Towner and Khanna [27] deduce $g_p = 11 \pm 2$. This result is model dependent. Note that our evaluation — given in Sec. VI — which essentially repeats this analysis but using here much improved wave functions, results in the quite different $g_p = 7.4 \pm 0.5$. Because of the model dependence involved, we have decided in this paper to quote results using the PCAC value of g_p, but give sufficient details — such as Eq. (22) — that the results can easily be modified for different values of g_p.

[1] E. K. Warburton, Phys. Rev. C **44**, 1024 (1991).
[2] E. K. Warburton and I. S. Towner, Phys. Lett. B **294**, 1 (1992).
[3] E. K. Warburton and I. S. Towner, Phys. Rpt. (to be published).
[4] D. J. Millener, D. E. Alburger, E. K. Warburton, and D. H. Wilkinson, Phys. Rev. C **26**, 1167 (1982).
[5] E. K. Warburton, D. E. Alburger, and D. H. Wilkinson, Phys. Rev. C **26**, 1186 (1982).
[6] E. K. Warburton, D. E. Alburger, and D. J. Millener, Phys. Rev. C **29**, 2281 (1984).
[7] C. A. Gagliardi, G. T. Garvey, N. Jarmie, and R. G. H. Robertson, Phys. Rev. C **27**, 1353 (1983).
[8] C. A. Gagliardi, G. T. Garvey, J. R. Wrobel, and S. J. Freedman, Phys. Rev. C **28**, 2423 (1983).
[9] L. A. Hamil, L. Lessard, H. Jeremie, and J. Chauvin, Z. Phys. A **321**, 439 (1985); H. Heath and G. T. Garvey, Phys. Rev. C **31**, 2190 (1985); T. Minamisono, K. Takeyama, T. Ishigai, H. Takeshima, Y. Nojiri, and K. Asahi, Phys. Lett. **130B**, 1 (1983); L. Palffy *et al.*, Phys. Rev. Lett. **34**, 212 (1975).
[10] E. K. Warburton, Phys. Rev. Lett. **66**, 1823 (1991); Phys. Rev. C **44**, 233 (1991).
[11] H. Behrens and W. Bühring, *Electron Radial Wave Functions and Nuclear Beta-Decay* (Clarendon, Oxford, England, 1982).
[12] G. E. Brown and A. M. Green, Nucl. Phys. **75**, 401 (1966).
[13] E. K. Warburton, B. A. Brown, and D. J. Millener, Phys. Lett. B **293**, 7 (1992).
[14] B. A. Brown, A. Etchegoyen, W. D. M. Rae, and N. S. Godwin, OXBASH, 1984 (unpublished).
[15] D. H. Glockner and R. D. Lawson, Phys. Lett. **53B**, 313 (1974).
[16] E. K. Warburton and B. A. Brown, Phys. Rev. C **46**, 923 (1992).
[17] E. K. Warburton, J. A. Becker, and B. A. Brown, Phys. Rev. C **41**, 1147 (1990).
[18] A. Hosaka, K.-I. Kubo, and H. Toki, Nucl. Phys. **A244**, 76 (1985).
[19] E. K. Warburton and D. J. Millener, Phys. Rev. C **39**, 1120 (1989).
[20] W. C. Haxton and C. Johnson, Phys. Rev. Lett. **65**, 1325 (1990).
[21] B. A. Brown and E. K. Warburton (unpublished).
[22] R. Machleidt, K. Holinde, and Ch. Elster, Phys. Rep. **149**, 1 (1987); R. Machleidt, Adv. Nucl. Phys. **19**, 189 (1989).
[23] T. T. S. Kuo (private communication).
[24] S. Nozawa, K. Kubodera, and H. Ohtsubo, Nucl. Phys. **A453**, 645 (1986).
[25] Particle Data Group, Phys. Rev. D **45**, S1 (1992).
[26] D. H. Wilkinson, in *Ecole d'Eté de Physique Théorique, Session XXX*, edited by R. Balian, M. Rho, and G. Ripka (North-Holland, Amsterdam, 1977), pp. 879–1017.
[27] I. S. Towner and F. C. Khanna, Nucl. Phys. **A372**, 331 (1981).
[28] A. H. Wapstra, G. Audi, and R. Hoekstra, At. Data Nucl. Data Tables **39**, 281 (1988); midstream update of the mass table, private communication from G. Audi (1990).
[29] D. H. Wilkinson and B. E. F. Macefield, Nucl. Phys. **A232**, 1 (1974).
[30] I. S. Towner, Annu. Rev. Nucl. Part. Sci. **36**, 115 (1986).
[31] In the previous treatments of Towner and Khanna [27] and Haxton and Johnson [20], an approximate expression, $a_S^\beta = 0.932[\frac{1}{3}(Q_\beta+1)+\xi]$, was used rather than the accurate formulation of Ref. [11] given in Eq. (7). Note that this approximation does not allow for the quite different contributions of the two terms in different transitions and thus is specific to this ^{16}N decay. Even so it does not allow for the state dependence of r_S^β. It should be noted that in previous treatments [10,32] r_S^β was labeled r_w'.
[32] E. K. Warburton, J. A. Becker, B. A. Brown, and D. J.

Millener, Ann. Phys. (N.Y.) **187**, 471 (1988).
[33] We use Edmonds' convention [34] for reduced matrix elements, triple overbars denote matrix elements reduced in both J and T, radial wave functions are positive at the origin, there is no i^l with the spherical harmonic, and the order of coupling is $\mathbf{l}\times\mathbf{s}$.
[34] A. R. Edmonds, *Angular Momentum in Quantum Mechanics* (Princeton University Press, Princeton, New Jersey, 1957).
[35] In "normal" units M_0^T is in $(\mathrm{MeV\,fm})^{-1}$. To convert to natural units multiply by $m_e\lambda\!\!\!^{-}_{Ce}$. Our convention of scaling matrix elements by $\lambda\!\!\!^{-}_{Ce}$ results in multiplication by $m_e\lambda\!\!\!^{-}_{Ce}{}^2$.
[36] H. de Vries, C. W. de Jager, and C. de Vries, At. Data Nucl. Data Tables **36**, 495 (1987).
[37] R. K. Bansal and J. B. French, Phys. Lett. **11**, 145 (1964).
[38] D. J. Millener and E. K. Warburton, in *Nuclear Shell Models*, edited by M. Vallieres and B. H. Wildenthal (World Scientific, Singapore, 1985), p. 365.
[39] I. S. Towner, Nucl. Phys. **A542**, 631 (1992).
[40] K. Kubodera, J. Delorme, and M. Rho, Phys. Rev. Lett. **40**, 755 (1978).
[41] P. Guichon, M. Giffon, J. Joesph, R. Laverrière, and C. Samour, Z. Phys. A **285**, 183 (1978); P. Guichon, M. Giffon, and C. Samour, Phys. Lett. **74B**, 15 (1978).
[42] B. A. Brown, W. A. Richter, and N. S. Godwin, Phys. Rev. Lett. **45**, 1681 (1980).
[43] This result was given on p. 340 of Ref. [27], however in that equation the sign of the last term was incorrect.
[44] E. K. Warburton, W. R. Harris, and D. E. Alburger, Phys. Rev. **175**, 1275 (1968).
[45] E. K. Warburton, in *Interactions and Structures in Nuclei*, edited by R. Blin-Stoyle and W. Hamilton (Adam Hilger, Bristol, England, 1988), pp. 81–88.
[46] It is difficult to make a detailed comparison between the results of Ref. [20] and the present ones because various approximations were made in Ref. [20] in the expressions for Λ_μ and Λ_β and not enough detail is given to separate the one-body and two-body contibutions.
[47] E. G. Adelberger and W. C. Haxton, Annu. Rev. Nucl. Part. Sci. **35**, 501 (1985).
[48] G. E. Brown and M. Rho, Phys. Lett. B **237**, 3 (1990).
[49] G. E. Brown and M. Rho, Phys. Rev. Lett. **66**, 2720 (1991).
[50] K. Kubodera and M. Rho, Phys. Rev. Lett. **67**, 3479 (1991).
[51] D. S. Armstrong *et al.*, Phys. Rev. C **46**, 1094 (1992).
[52] M. Döbeli *et al.*, Phys. Rev. C **37**, 1633 (1988).
[53] F. Ajzenberg-Selove, Nucl. Phys. **A375**, 1 (1982).